Conductivity Measurements at the Interface Between the Sintered Conductor and Dielectric Substrate at Microwave Frequencies

Akira Nakayama, Yoshitake Terashi, Hiroshi Uchimura, and Atsuomi Fukuura, *Member, IEEE*

***Abstract*—A novel measuring technique of the effective conductivity at microwave frequencies for both the sintered conductor surface and the interface between conductor and dielectric materials was developed. In the measurement, a dielectric rod resonator is placed between two dielectric plates, one side of which is coated with a sintered conductor. For measuring the surface conductivity, the dielectric rod is sandwiched by the conductor side of the plates. On the other hand, for measuring the interface conductivity, the dielectric rod is sandwiched by the dielectric side of the plates. By the configuration, only interface conductivity contributes to the conducting loss of the resonator, thus allowing the measurement of the interface conductivity. Using the new technique, the frequency dependence of both the surface and interface conductivity of a sintered copper, formed on a glass ceramic substrate by the co-firing technique, was investigated in the frequency range from 11 to 34 GHz. It was confirmed that the values of interface conductivity of the sintered copper were smaller than the values of the surface conductivity.**

***Index Terms*—Complex permittivity, dielectric rod resonator, glass ceramic substrate, interface conductivity, microwave measurement, sapphire, sintered copper.**

I. Introduction

THE attenuation of planar transmission lines, such as striplines, microstrip lines, and coplanar lines, are determined by conducting, dielectric, and radiation losses. It is commonly known that the conducting loss is the major factor affecting the overall attenuation of those planar transmission lines at microwave frequencies. In the microwave range, electric current is concentrated within a skin depth of the order of micrometer thickness. This is taken into account as actual skin resistance, specifically the surface resistance R_s and the interface resistance R_i, or effective surface conductivity σ_s and interface conductivity σ_i. Evaluation of an accurate value of the effective conductivity becomes very important for conductor pattern designing and conductor formation process development. When focusing on planar transmission lines, σ_i is particularly important, because the microwave current is more concentrated on the dielectric side, rather than the air side, of the conductor due to a high dielectric constant. However, there have been few efforts to measure the effective conductivity, particularly the interface conductivity, of a sintered conductor formed on the ceramic substrate, while several studies have been carried out for measuring the complex permittivity of ceramic substrates [1]–[7].

Tanaka *et al.* [8] presented a technique for measuring the σ_i at microwave frequency using stripline resonators. They have separately measured the conducting and dielectric losses of printed circuit boards, using several stripline resonators of different dimensions. The result of their measurements indicated that the effective conductivity of the industrial copper foil, widely used for cladding, was significantly affected by the surface roughness of its bonding side.

Multilayered ceramic substrates and packages, including many transmission lines, are made by co-firing with the conductor. In this case, the interface between the conductor and ceramics usually has roughness, a reaction layer, and a concentration of glass material, depending on the co-firing process and the compositions of the ceramic and conductor materials. Such interfaces usually have low conductivity. To design the microwave circuit and develop the process technology of the co-firing, an accurate and simple measurement technique is needed for σ_i at microwave frequencies.

In this paper, we propose a novel technique for measuring both the σ_s and σ_i at microwave frequencies. The technique is based on the dielectric resonator method, a popular technique for measuring dielectric constants at microwave frequency. Using the proposed technique, we have investigated the frequency dependence of both σ_s and σ_i of a sintered copper formed on a glass ceramic substrate using the co-firing technique in the frequency range from 11 to 34 GHz.

II. Measurement Principle

A. Conductivity Measurement

Configurations of the TE_{011} mode dielectric rod resonator for measuring surface conductivity σ_s and the $\mathrm{TE}_{01\delta}$ mode resonator for measuring interface conductivity σ_i are shown in Fig. 1. Fig. 1 also illustrates typical electric and magnetic fields for each TE mode resonator by solid and broken lines, respectively. The resonators consist of a dielectric rod and two test samples of circular dielectric substrate, covered with a sintered conductor at one side. Here, the sintered conductor is supposed to be much thicker compared with the skin depth. The rod has diameter D, height H, relative permittivity $\varepsilon'_{\mathrm{rod}}$, and loss tangent $\tan\delta_{\mathrm{rod}}$. The corresponding sizes and dielectric constants of the dielectric substrate are presented as d, t, $\varepsilon'_{\mathrm{sub}}$, and $\tan\delta_{\mathrm{sub}}$. For

Manuscript received September 10, 2001.

A. Nakayama, Y. Terashi, and H. Uchimura are with the R&D Center Kagoshima, Kyocera Corporation, Kagoshima 899-4312, Japan (e-mail: Akira_Nakayama@rdg.kyocera.co.jp).

A. Fukuura is with the R&D Center Keihanna, Kyocera Corporation, Kyoto 619-0237, Japan.

Publisher Item Identifier 10.1109/TMTT.2002.800382.

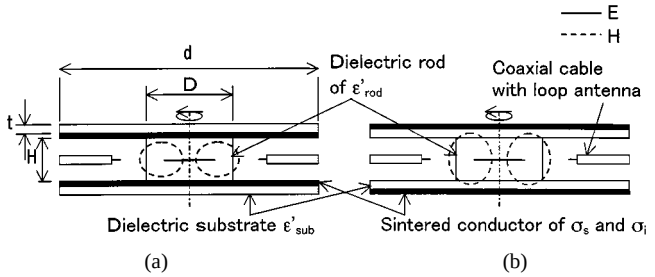

Fig. 1. Configurations of the TE_{011} and $\mathrm{TE}_{01\delta}$ mode resonators for measurements of effective surface conductivity σ_s and interface conductivity σ_i. Typical electric and magnetic fields are illustrated. (a) TE_{011} mode resonator for σ_s. (b) $\mathrm{TE}_{01\delta}$ mode resonator for σ_i.

measurement of σ_s, both ends of the rod are short-circuited by the surfaces of the sintered conductor of the sample, as shown in Fig. 1(a). In such a configuration, only the σ_s of the conductor contributes to the conducting loss in the TE_{011} mode resonator. For measurement of σ_i, the rod is sandwiched by the dielectric sides, as shown in Fig. 1(b). In this configuration, only σ_i can contribute to the conducting loss in the $\mathrm{TE}_{01\delta}$ mode resonator, allowing the measurement of σ_i. By unloaded Q measurements of the two resonators, σ_s and σ_i can be determined separately, when the conductor is much thicker than the skin depth.

Moreover, it is important that the dielectric loss arising from the substrate is very small in our $\mathrm{TE}_{01\delta}$ resonator. The electric field in the $\mathrm{TE}_{01\delta}$ mode vanishes on the both conductors and reaches a maximum at the central transverse plane of the sapphire rod. The electric field is very small in the substrates, positioned at the both ends of the dielectric rod. Accordingly, the effect of the dielectric loss by the substrate on the Q_u of the $\mathrm{TE}_{01\delta}$ resonator is relatively small, compared with the conductor loss by interface conductivity and the dielectric loss of the rod. The interface conductivity can be determined without serious influence of the dielectric loss by the substrate.

The value of σ_s is calculated from the measured values of the resonant frequency f_0 and the unloaded Q, Q_u of the TE_{011} mode resonator shown in Fig. 1(a). The value of σ_i is calculated from those of the $\mathrm{TE}_{01\delta}$ mode resonator shown in Fig. 1(b). When d is infinitely large, radiation loss can be neglected and Q_u of the resonator in Fig. 1(a) is determined from the dielectric loss by the rod and the conductor loss by the surface resistance as follows:

$$1/Q_{u,\,s} = P_{\mathrm{erod},\,s}\tan\delta_{\mathrm{rod}} + R_s/G_s. \tag{1}$$

In the same way, Q_u of the resonator in Fig. 1(b) is determined from the dielectric losses by the rod and substrate, and conductor loss by the interface resistance as follows:

$$1/Q_{u,\,i} = P_{\mathrm{erod},\,i}\tan\delta_{\mathrm{rod}} + P_{\mathrm{esub},\,i}\tan\delta_{\mathrm{sub}} + R_i/G_i. \tag{2}$$

Here, the subscripts s and i indicate the resonator shown in Fig. 1(a) and (b), respectively. The P_{erod} in (1) is a partial electric energy filling factor [9] of the dielectric rod and P_{esub} in (2) is that of the dielectric substrate, defined by

$$P_{\mathrm{erod}} = \frac{W_{\mathrm{erod}}}{W_{et}} = \frac{\varepsilon'_{\mathrm{rod}}\iiint_{V\mathrm{rod}}|\mathbf{E}|^2\,dv}{\iiint_{Vt}\varepsilon'(v)|\mathbf{E}|^2\,dv} \tag{3}$$

$$P_{\mathrm{esub}} = \frac{W_{\mathrm{esub}}}{W_{et}} = \frac{\varepsilon'_{\mathrm{sub}}\iiint_{V\mathrm{sub}}|\mathbf{E}|^2\,dv}{\iiint_{Vt}\varepsilon'(v)|\mathbf{E}|^2\,dv} \tag{4}$$

where W_{erod} is the electric energy stored in the rod, W_{esub} is that stored in the substrate and W_{et} is the total electric energy stored in the resonator structure. The $\varepsilon'(v)$ generally represents relative permittivity in the resonant structure. The G in (1) and (2) is a geometric factor of the resonator [9], defined by

$$G = \frac{\omega\mu_0\iiint_{Vt}|\mathbf{H}|^2\,dv}{\iint_s|\mathbf{H}_t|^2\,ds} \tag{5}$$

where $\iint_s|\mathbf{H}_t|^2\,ds$ is a surface integration of the magnetic field at the surface side for G_s in (1) or the interface side for G_i in (2) of a sintered conductor. Furthermore, the relation of R_s and σ_s, or R_i and σ_i is given by

$$R_{s(i)} = \sqrt{\frac{\omega_{s(i)}\mu}{2\sigma_{s(i)}}} \tag{6}$$

where μ is the permeability of the sintered conductor.

Values of G_s and $P_{\mathrm{erod},\,s}$ are calculated by exact equations [10], [11], as follows:

$$P_{\mathrm{erod},\,s} = 1/A \tag{7}$$

$$G_s = B/A \tag{8}$$

$$A = 1 + \frac{W}{\varepsilon'} \tag{9}$$

$$B = \ell^2\left(\frac{\lambda_0}{2H}\right)^3\frac{1+W}{30\pi^2\varepsilon'}, \qquad \ell = 1, 2, \ldots \tag{10}$$

where

$$\lambda_0 = c/f_0 \tag{11}$$

$$W = \frac{J_1^2(u)}{K_1^2(v)}\,\frac{K_0(v)K_2(v) - K_1^2(v)}{J_1^2(u) - J_0(u)J_2(u)} \tag{12}$$

$$v^2 = \left(\frac{\pi D}{\lambda_0}\right)^2\left[\left(\frac{\ell\lambda_0}{2H}\right)^2 - 1\right] \tag{13}$$

$$u\,\frac{J_0(u)}{J_1(u)} = -v\,\frac{K_0(v)}{K_1(v)}. \tag{14}$$

Here, A and B are given by Hakki and Coleman [10], for determination of $\tan\delta$ using the $\mathrm{TE}_{0m\ell}$ mode dielectric rod resonator. c is the velocity of light in the vacuum. J and K are the first- and the second-order modified Bessel functions. For any value of v, the mth solution u exists between u_{0m} and u_{1m} in (14), where $J_0(u_{0m}) = 0$ and $J_1(u_{1m}) = 0$. In this study, the values of $P_{\mathrm{erod},\,s}$ and G_s are calculated from the first solution u of (14) and by setting $\ell = 1$ in (10) and (13), since these parameters correspond to the TE_{011} mode.

On the other hand, the G_i, $P_{\mathrm{erod},\,i}$ and $P_{\mathrm{esub},\,i}$ are obtained by axis symmetric FEM calculation. Accuracy of the FEM analysis is described in Section IV.

Equations (1) and (2) are derived by assuming that the plate sample has infinitely large d. In practice, a suitable finite size of the sample plates is permitted, since the TE-mode electromagnetic field outside the rod rapidly decreases in the radial direction. We have analytically estimated the required value of the diameter ratio $S = d/D$, as a function of a thickness ratio of the substrate to the rod t/H and $\varepsilon'_{\mathrm{sub}}$ (see the Appendix).

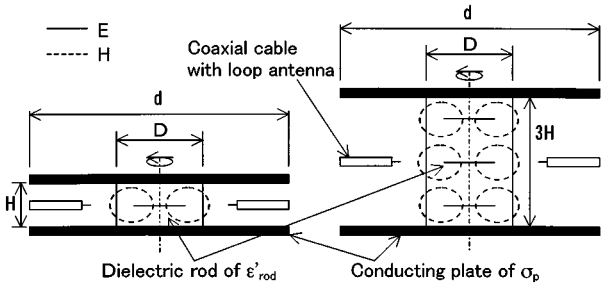

Fig. 2. Structure of TE_{011} and TE_{013} mode resonators for measurements of relative permittivity $\varepsilon'_{\mathrm{rod}}$ and loss tangent $\tan\delta_{\mathrm{rod}}$ of dielectric rods. Typical electric and magnetic fields are illustrated. (a) TE_{011} mode resonator. (b) TE_{013} mode resonator.

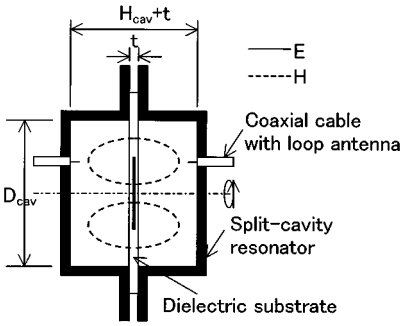

Fig. 3. Structure of TE_{011} mode cavity resonators for measurements of relative permittivity $\varepsilon'_{\mathrm{sub}}$ and loss tangent $\tan\delta_{\mathrm{sub}}$ of the dielectric substrate. Typical electric and magnetic fields are illustrated.

B. Complex Permittivity Measurement

For measurements of σ_s and σ_i, relative permittivity ε' and loss tangent $\tan\delta$ of the dielectric rod and substrate should first be determined. The $\varepsilon'_{\mathrm{rod}}$ and $\tan\delta_{\mathrm{rod}}$ were measured by a dielectric rod resonator method [10], [11]. In the resonator used for this method, both ends of the dielectric rod are short-circuited by the conducting plate. When both $\tan\delta_{\mathrm{rod}}$ and effective conductivity of the conducting plates σ_p are unknown, a pair of TE_{011} and $\mathrm{TE}_{01\ell}$ mode dielectric rod resonators must be used [11]. The two resonators are required to have the same values of $\varepsilon'_{\mathrm{rod}}$ and $\tan\delta_{\mathrm{rod}}$. Furthermore, same conducting plates are used in these resonators. ℓ is commonly set to $\ell = 3$ as shown in Fig. 2. Both dielectric rods have the same diameter D and the TE_{013} mode rod is three times the height of the TE_{011} mode rod. When the diameter of the conducting plate d is larger than four times the rod diameter D, the conducting plate can be assumed to be infinitely large. From resonant frequency f_0 measurements of each mode, $\varepsilon'_{\mathrm{rod}}$ is calculated by

$$\varepsilon'_{\mathrm{rod}} = \left(\frac{\lambda_0}{\pi D}\right)^2 (u^2 + v^2) + 1 \tag{15}$$

where v^2 and u^2 are given by (13) and (14). Next, $\tan\delta_{\mathrm{rod}}$ and σ_p are obtained from Q_u measurements of both mode resonators by the following equations:

$$1/Q_{u1} = P_{erod1}\tan\delta_{\mathrm{rod}} + R_p/G_1 \tag{16}$$

$$1/Q_{u3} = P_{erod3}\tan\delta_{\mathrm{rod}} + R_p/G_3 \tag{17}$$

$$R_p = \sqrt{\frac{\omega\mu}{2\sigma_p}} \tag{18}$$

where R_p is the skin resistance of the conducting plate. Subscripts 1 and 3 indicate the TE_{011} and TE_{013} mode resonators, respectively. P_{erod1} and G_1 are calculated by (7) and (8), since those values are the same as $P_{\mathrm{erod},\,s}$ and G_s, respectively. P_{erod3} and G_3 are also calculated by (7) and (8), when ℓ is set to $\ell = 3$ for calculations of (9)–(14). When both dielectric rods precisely have the same diameter D and the TE_{013} mode rod is precisely three times the height of the TE_{011} mode rod, $P_{\mathrm{erod1}} = P_{\mathrm{erod}}$ and $G_1 = 3G_3$ are obvious from (3) and (5). On the other hand, if σ_p is known, $\tan\delta_{\mathrm{rod}}$ can be determined from measurements of the TE_{011} mode resonator, using (16).

$\varepsilon'_{\mathrm{sub}}$ and $\tan\delta_{\mathrm{sub}}$ were measured by a split-cavity resonator method [1]–[4] at 10–20 GHz, using substrates without a sintered conductor. In the split-cavity resonator method, the dielectric substrate of thickness t is placed between the sections of the cavity of internal diameter D_{cav} and height H_{cav}, as shown in Fig. 3. The $\varepsilon'_{\mathrm{sub}}$ and $\tan\delta_{\mathrm{sub}}$ are determined by resonant frequency f_0 and unloaded Q, Q_u, measurements. In this study, $\varepsilon'_{\mathrm{sub}}$ and $\tan\delta_{\mathrm{sub}}$ were calculated by equations described in the literatures[1], [2].

At frequency above 20 GHz, ε'_{sub} and $\tan\delta_{sub}$ were measured by the rod resonator method above-mentioned, using rod samples cut out from the substrate and conducting plate of known conductivity.

III. Equipment

The dielectric rod resonators for measuring σ_s, σ_i, $\varepsilon'_{\mathrm{rod}}$, and $\tan\delta_{\mathrm{rod}}$, and the cavity resonator for measuring $\varepsilon'_{\mathrm{sub}}$ and $\tan\delta_{\mathrm{sub}}$ were undercoupled equally to input and output loops on the top of semi-rigid cables. The insertion loss IL_0 at f_0 was adjusted to around 30 dB. f_0, the half-power bandwidth $f_2 - f_1$, and IL_0 were measured using the HP Network Analyzer 8757C by the swept-frequency method. Q_u is obtained by

$$Q_u = \frac{f_o}{f_2 - f_1} \Big/ \left(1 - 10^{-IL_0/20}\right). \tag{19}$$

IV. Results and Discussion

A. Complex Permittivity Measurement

The dielectric rod used for σ_s and σ_i measurements is required to have small $\tan\delta$, since the dielectric loss degrades the accuracy of the measurements. We used single-crystal sapphire rods with a rotational axis parallel to the C axis, because of its extremely small $\tan\delta$.

Complex permittivity of the sapphire rod was obtained by the dielectric rod resonator method [10], [11]. The copper plates, with a mirror surface of about 0.03-μm roughness, were set on both ends of the rod for short-circuiting in the measurements, by no applied pressure. The effective relative conductivity σ_{pr} of these plates and $\tan\delta_{\mathrm{rod}}$ of the sapphire rods were simultaneously obtained from Q_u measurements of TE_{011} and TE_{013} mode resonators [11]. Table I and Fig. 4 show the measured values of $\varepsilon'_{\mathrm{rod}}$ and $\tan\delta_{\mathrm{rod}}$, perpendicular to the C axis, of the sapphire rods used in this study, at 298 K and in the frequency range from 11 to 34 GHz. The values of σ_{pr}, normalized by the standard copper conductivity $\sigma_0 = 5.8 \times 10^7$ S/m, of the copper plates are also listed in Table I. The values of $\varepsilon'_{\mathrm{rod}}$ of the sapphire

TABLE I
MEASUREMENTS OF THE RELATIVE PERMITTIVITY $\varepsilon'_{\rm rod}$ AND LOSS TANGENT $\tan\delta_{\rm rod}$ OF SAPPHIRE RODS, WHICH ARE VALUES PERPENDICULAR TO THE C AXIS OF THE SAPPHIRE CRYSTAL. RELATIVE EFFECTIVE CONDUCTIVITY σ_{pr}. VALUES OF COPPER PLATES USED FOR MEASURING $\varepsilon'_{\rm rod}$ AND $\tan\delta_{\rm rod}$ ARE ALSO LISTED. THOSE ARE NORMALIZED BY A CONDUCTIVITY OF $\sigma_0 = 5.8 \times 10^7$ [S/m] OF THE STANDARD COPPER

No.	Diameter of rod D (mm)	Height of rod H (mm)	Resonant frequency f_0 (GHz)	Unloaded Q Q_u	Relative permittivity ε'_{rod}	Loss tangent $\tan\delta_{rod}$ (10^{-5})	Conductivity of Cu-plate σ_{pr} (%)
R1-1	11.814	5.639	11.7886	6710	9.416	1.16	91.5
TE_{011}	±0.001	±0.001	±0.0006	±17	±0.002	±0.05	±1.0
R1-3	11.818	16.645	11.9209	17137	9.390		
TE_{013}	±0.001	±0.006	±0.0003	±62	±0.004		
R2-1	8.005	3.724	17.679	5216	9.411	1.78	89.9
TE_{011}	±0.001	±0.001	±0.004	±17	±0.006	±0.08	±1.3
R2-3	8.005	11.171	17.690	13222	9.400		
TE_{013}	±0.001	±0.001	±0.001	±91	±0.002		
R3-1	6.504	3.015	21.821	4667	9.399	2.25	91.7
TE_{011}	±0.001	±0.001	±0.002	±29	±0.004	±0.10	±2.1
R3-3	6.508	9.058	21.796	11610	9.399		
TE_{013}	±0.001	±0.001	±0.001	±76	±0.002		
R4-1	5.111	2.426	27.340	4188	9.417	2.71	90.0
TE_{011}	±0.001	±0.001	±0.009	±53	±0.008	±0.20	±4.4
R4-3	5.110	7.273	27.366	10256	9.409		
TE_{013}	±0.002	±0.001	±0.001	±79	±0.003		
R5-1	4.001	2.008	33.769	3773	9.419	3.24	82.9
TE_{011}	±0.001	±0.001	±0.003	±22	±0.006	±0.12	±1.8
R5-3	3.998	6.022	33.807	9123	9.407		
TE_{013}	±0.001	±0.001	±0.001	±56	±0.003		

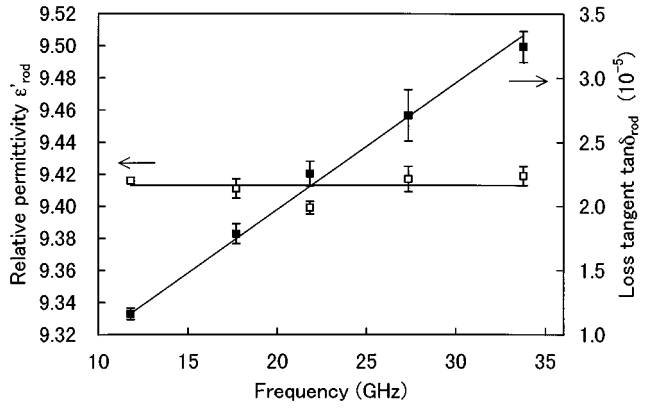

Fig. 4. Frequency dependence of the sapphire rod relative permittivity $\varepsilon'_{\rm rod}$ and loss tangent $\tan\delta_{\rm rod}$, perpendicular to the C axis.

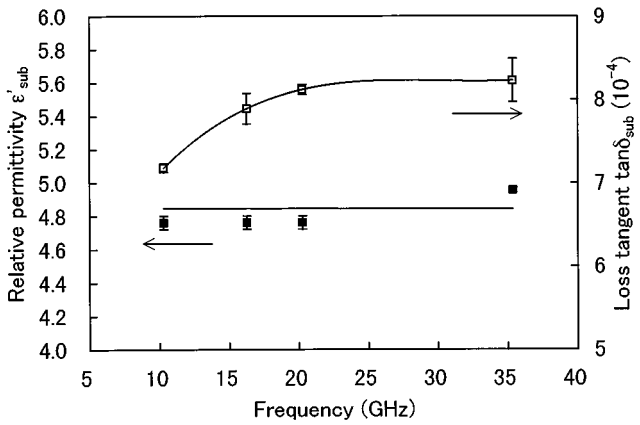

Fig. 5. Frequency dependence of the glass ceramic substrate relative permittivity $\varepsilon'_{\rm sub}$ and loss tangent $\tan\delta_{\rm sub}$.

are about 9.41 and the frequency dependence of $\tan\delta_{\rm rod}$ of the sapphire is expressed by frequency/$\tan\delta = 1.01 \times 10^6$ GHz. These values have good agreement with the reported dielectric properties of sapphire perpendicular to c-axis, that is, $\varepsilon' = 9.4$ and frequency/$\tan\delta = 1.0 \times 10^6$ GHz at room temperature [12]. Table I and Fig. 4 also show random errors of measurements. The random errors of $\varepsilon'_{\rm rod}$, $\tan\delta_{\rm rod}$ and σ_{pr} are evaluated by

$$(\Delta\varepsilon_{\rm rod})^2 = (\Delta\varepsilon_{f0})^2 + (\Delta\varepsilon_D)^2 + (\Delta\varepsilon_H)^2 \quad (20)$$

$$(\Delta\tan\delta_{\rm rod})^2 = (\Delta\tan\delta_{Qu1})^2 + (\Delta\tan\delta_{Qu3})^2 \quad (21)$$

$$(\Delta\sigma_{pr})^2 = (\Delta\sigma_{Qu1})^2 + (\Delta\sigma_{Qu3})^2 \quad (22)$$

where $\Delta\varepsilon_{f0}$, $\Delta\varepsilon_D$, and $\Delta\varepsilon_H$ are errors of $\varepsilon'_{\rm rod}$ induced by the standard deviations of f_0, rod diameter D, and height H. In the same way, $\Delta\tan\delta_{Qu1}$, $\Delta\tan\delta_{Qu3}$, $\Delta\sigma_{Qu1}$, and $\Delta\sigma_{Qu3}$ are defined as errors induced by the standard deviations of Q_{u1} or Q_{u3}. Here, Q_{u1} and Q_{u3} are unloaded Q values of the $\rm TE_{011}$ and $\rm TE_{013}$ mode resonators, respectively.

To make a test sample, we used a new glass ceramic material [13] developed by Kyocera. Fig. 5 and Table II show the frequency dependence of dielectric properties of the new material that relative permittivity $\varepsilon'_{\rm sub}$ is 4.8 ± 0.1 and dielectric loss tangent $\tan\delta_{\rm sub}$ increases from 7×10^{-4} to 8×10^{-4} with increasing frequency from 10 to 35 GHz. This slope in frequency

TABLE II
MEASUREMENTS OF THE RELATIVE PERMITTIVITY $\varepsilon'_{\rm sub}$ AND LOSS TANGENT $\tan\delta_{\rm sub}$ OF A NEW GLASS CERAMIC SUBSTRATE. (a) VALUES OF $\varepsilon'_{\rm sub}$ AND $\tan\delta_{\rm sub}$ OBTAINED BY SPLIT-CAVITY RESONATOR AT 10, 16, AND 20 GHz, USING PLATE SAMPLE. (b) VALUES OF $\varepsilon'_{\rm sub}$ AND $\tan\delta_{\rm sub}$ OBTAINED BY A DIELECTRIC ROD RESONATOR AT 35 GHz, USING THE ROD SAMPLE

Sample and mode	Thick. (mm)	Resonant frequency f_0 (GHz)	Unloaded Q Q_u	Relative permittivity ε'_{sub}	Loss tangent $\tan\delta_{sub}$ (10^{-4})	Diameter and height of Cavity D_{cav} (mm)	H_{cav} (mm)	Conductivity of Cu-cavity σ_{cavr} (%)
Plate TE_{011}	0.965 ±0.08	10.287 ±0.003	3313 ±22	4.76 ±0.04	7.18 ±0.05	35.050 ±0.001	25.079 ±0.001	86.1 ±2.4
		16.253 ±0.001	2047 ±43	4.76 ±0.04	7.89 ±0.18	20.057 ±0.002	14.327 ±0.003	81.8 ±1.8
		20.271 ±0.011	1689 ±12	4.76 ±0.04	8.12 ±0.06	15.034 ±0.001	10.829 ±0.001	72.9 ±1.9

(a)

Sample and mode	Diameter D (mm)	Height H (mm)	Resonant frequency f_0 (GHz)	Unloaded Q Q_u	Relative permittivity ε'_{sub}	Loss tangent $\tan\delta_{sub}$ (10^{-4})	Conductivity of Cu-plate σ_{pr} (%)
Rod TE_{011}	7.323 ±0.004	2.244 ±0.003	35.371 ±0.037	938 ±23	4.956 ±0.014	8.2 ±0.3	87 ±2

(b)

dependence of $\tan\delta_{\rm sub}$ is very small compared with conventional glass ceramics or other ceramic substrate. The measured values at 10, 16, and 20 GHz were obtained by the split-cavity resonator [1]–[4], using a plate sample. Those at 35 GHz were obtained by the dielectric rod resonator [10], [11], using a rod sample. Random errors of $\varepsilon'_{\rm sub}$, $\tan\delta_{\rm sub}$ by the split-cavity resonator evaluated by

$$(\Delta\varepsilon_{\rm sub})^2=(\Delta\varepsilon_{f0})^2+(\Delta\varepsilon_t)^2+(\Delta\varepsilon_{D\rm cav})^2+(\Delta\varepsilon_{H\rm cav})^2 \tag{23}$$

$$(\Delta\tan\delta_{\rm sub})^2=(\Delta\tan\delta_{Qu})^2+(\Delta\tan\delta_{\sigma\rm cav})^2 \tag{24}$$

where $\Delta\varepsilon_{f0}$, $\Delta\varepsilon_t$, $\Delta\varepsilon_{D\rm cav}$, and $\Delta\varepsilon_{H\rm cav}$ are the errors of $\varepsilon'_{\rm sub}$ induced by the standard deviations of f_0, plate thickness t, internal diameter $D_{\rm cav}$, and height $H_{\rm cav}$ of the cavity. In the same way, $\Delta\tan\delta_{Qu}$ and $\Delta\tan\delta_{{\rm cav}\sigma}$ are defined as the errors by the standard deviations of Q_u and effective conductivity of cavity $\sigma_{\rm cav}$. Furthermore, random errors of $\varepsilon'_{\rm sub}$, $\tan\delta_{\rm sub}$ by the dielectric rod resonator evaluated by

$$(\Delta\varepsilon_{\rm sub})^2=(\Delta\varepsilon_{f0})^2+(\Delta\varepsilon_D)^2+(\Delta\varepsilon_H)^2 \tag{25}$$

$$(\Delta\tan\delta_{\rm sub})^2=(\Delta\tan\delta_{Qu})^2+(\Delta\tan\delta_{\sigma p})^2 \tag{26}$$

where $\Delta\varepsilon_{f0}$, $\Delta\varepsilon_D$, and $\Delta\varepsilon'_H$ are the same as those in (20). $\Delta\tan\delta_{Qu}$ and $\Delta\tan\delta_{\sigma p}$ are the errors by the standard deviations of Q_u and effective conductivity σ_p of the copper plate used in the rod resonator method.

B. Calculation of Parameters for σ_i Measurements

For σ_i measurements, a partial electric energy filling factor of the sapphire rod and glass ceramic substrate, $P_{{\rm erod},i}$ and $P_{{\rm esub},i}$, and geometrical factor G_i corresponding to each dielectric rod (R1-1∼R5-1) were obtained by axis symmetric FEM. In the analysis model of the resonator, a side wall of the conductor was placed at diameter d. The diameter ratio of the substrate to the rod, $S=d/D$, was set to 5, to let the electromagnetic field be negligibly small near the side wall.

Calculated results for the dielectric rod R1-1 are shown in Fig. 6, as a function of the thickness t and relative permittivity $\varepsilon'_{\rm sub}$ of the substrate. The calculation model is also shown in Fig. 6(a). Fig. 6 shows some basic tendencies. The partial electric energy filling factor of rod $P_{{\rm erod},i}$ decreases with increasing t and $\varepsilon'_{\rm sub}$. That of substrate $P_{{\rm esub},i}$, on the contrary, increases with increasing t and $\varepsilon'_{\rm sub}$. These dependencies on t and $\varepsilon'_{\rm sub}$ are reasonably understood from the definition of $P_{\rm erod}$ and $P_{\rm esub}$ by (3) and (4). On the other hand, $1/G_i$ decreases with increasing t and increases with increasing $\varepsilon'_{\rm sub}$. When t increases, the conductor goes away from the dielectric rod where the electromagnetic field is concentrated. In this case, magnetic field intensity at the conductor decreases and $1/G_i$ also decreases. When $\varepsilon'_{\rm sub}$ increases, the electromagnetic field concentrated in the rod relatively spreads to the substrate. Then, the magnetic field intensity at the conductor increases and $1/G_i$ also increases.

C. Conductivity Measurement

Values of σ_s and σ_i of a sintered copper 10-μm thick formed on the glass ceramic substrate by co-firing were inferred from unloaded Q measurements of $\rm TE_{011}$ and $\rm TE_{01\delta}$ mode sapphire resonators. The sintering temperature was less than 1000 °C. The substrate was 45-mm square with thickness $t=0.136$ mm with about 1-μm surface roughness, and the sapphire rods of R1-1∼R5-1 with ends of about 0.01-μm surface roughness, shown in Table I, were used for measurements in the frequency range from 11 to 34 GHz. Using FEM analysis of the measurement configurations (see the Appendix), it was found that the

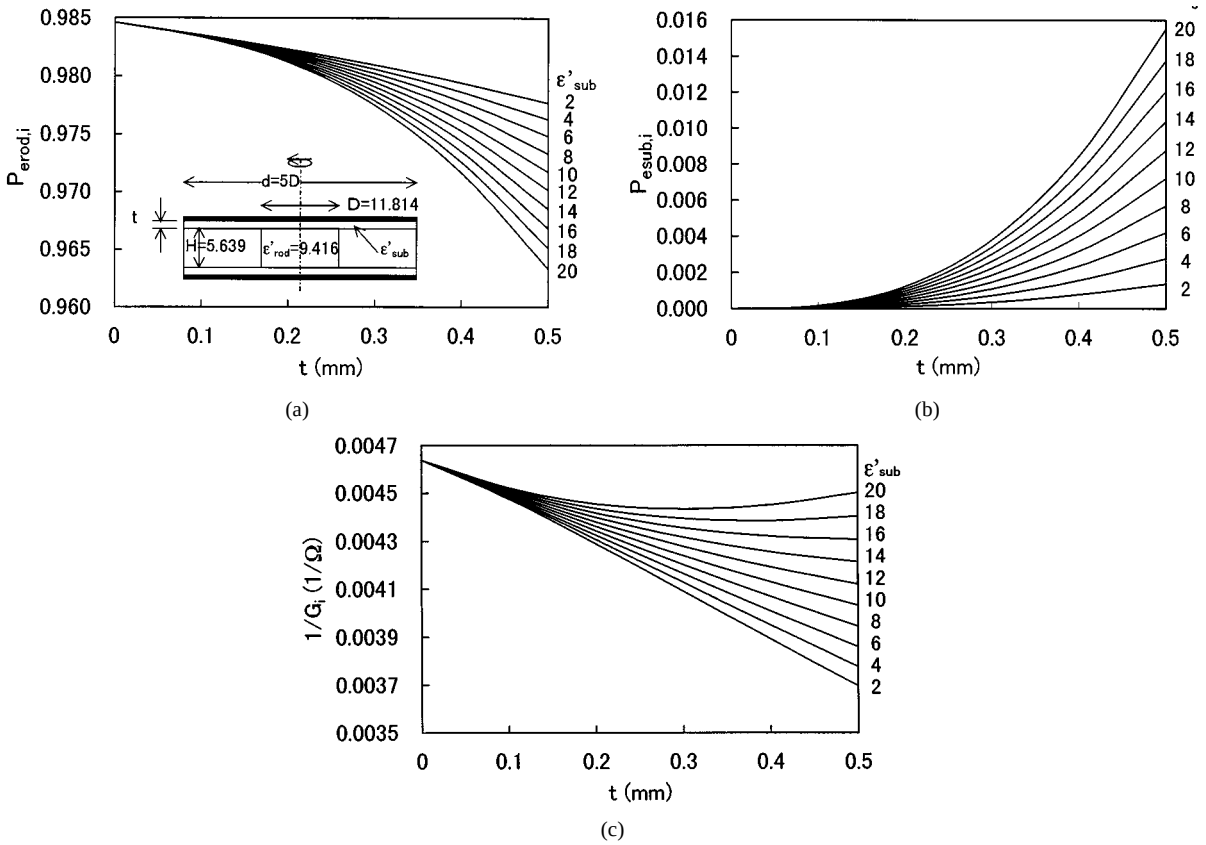

Fig. 6. Calculations of partial electric energy filling factor of sapphire rod and substrate, $P_{\mathrm{crod},\,i}P_{\mathrm{csub},\,i}$, and geometric factor G_i, for σ_i measurements by sapphire rod R1-1, using FEM analysis. (a) $P_{\mathrm{crod},\,i}$ (b) $P_{\mathrm{csub},\,i}$. (c) G_i.

effect of radiation losses is below a typical resolution limit of our measurements and are therefore negligibly small, under the condition of $S = d/D$ and t/H in Table III.

Values of the σ_s and σ_i were obtained by unloaded Q measurements of TE_{011} and $\mathrm{TE}_{01\delta}$ mode sapphire resonator, respectively, using (1) and (2). In the calculation, $\varepsilon'_{\mathrm{rod}}$ and $\tan\delta_{\mathrm{rod}}$ as a function of frequency showed in Table I were used. A typical complex permittivity of substrate material, $\varepsilon'_{\mathrm{sub}} = 4.8$ and $\tan\delta_{\mathrm{sub}} = 8 \times 10^{-4}$, were also used for the σ_s and σ_i calculations. Fig. 7 shows an example of resonant peaks in the measurements. Results of the σ_s and σ_i measurements are shown in Table II, with corresponding R_s and R_i. Here, σ_{sr} and σ_{ir} are listed as the relative conductivity of σ_s and σ_i normalized by the standard copper conductivity $\sigma_0 = 5.8 \times 10^7$ S/m. Fig. 8 shows the frequency dependencies of σ_{sr} and σ_{ir}. We can see that values of σ_{ir} are smaller than those of σ_{sr}, and both values of σ_{sr} and σ_{ir} degrade as the frequency increases. The smaller values of σ_i are considered to come from roughness and a reaction layer on the interface between the sintered copper and the substrate. Table IV and Fig. 8 also show random errors of measurements. The evaluation of the random errors of σ_{sr} and σ_{ir} are described in the next section.

D. Accuracy of Measurement

Random measurement errors of σ_{sr} are determined by errors of Q_u and $\tan\delta_{\mathrm{rod}}$. In the case of σ_{ir}, the error of $\tan\delta_{\mathrm{sub}}$ should be also considered. The mean-square error $\Delta\sigma_{sr}$ and $\Delta\sigma_{ir}$ are estimated from the standard deviations of Q_u, $\tan\delta_{\mathrm{rod}}$, and $\tan\delta_{\mathrm{sub}}$ by

$$(\Delta\sigma_{sr})^2 = (\Delta\sigma_{Qu})^2 + (\Delta\sigma_{\tan\delta\mathrm{rod}})^2 \tag{27}$$

$$(\Delta\sigma_{ir})^2 = (\Delta\sigma_{Qu})^2 + (\Delta\sigma_{\tan\delta\mathrm{rod}})^2 + (\Delta\sigma_{\tan\delta\mathrm{sub}})^2 \tag{28}$$

where $\Delta\sigma_{Qu}$, $\Delta\sigma_{\tan\delta\mathrm{rod}}$, and $\Delta\sigma_{\tan\delta\mathrm{sub}}$ are the errors of σ_{sr} or σ_{ir} by standard deviations of Q_u, $\tan\delta_{\mathrm{rod}}$, and $\tan\delta_{\mathrm{sub}}$. The standard deviation of $\tan\delta_{\mathrm{sub}}$ was assumed to be 1×10^{-4}, comparable to the typical uncertainty and the variation in the frequency range from 10 to 35 GHz of the substrate material used in this study, as shown in Fig. 5. The other standard deviations were determined from each measurement.

The values of $\Delta\sigma_{sr}$ and $\Delta\sigma_{ir}$ obtained by (27) and (28) are shown in Table III, with errors of skin resistance, ΔR_s and ΔR_i. $\Delta\sigma_{sr}$ and $\Delta\sigma_{ir}$ were estimated to be within 5%. To show typical values of $\Delta\sigma_{Qu}$, $\Delta\sigma_{\tan\delta\mathrm{rod}}$, and $\Delta\sigma_{\tan\delta\mathrm{sub}}$, those in measurements at 17–22 GHz are shown in Table IV. Table IV indicates that $\Delta\sigma_{Qu}$ and $\Delta\sigma_{\tan\delta\mathrm{rod}}$ are dominant errors. In contrast, $\Delta\sigma_{\tan\delta\mathrm{sub}}$ by $\Delta\tan\delta_{\mathrm{sub}} = 1 \times 10^{-4}$ is negligibly small, since the partial electric energy filling factor of the substrate P_{esub} is very small compared with that of rod P_{erod}. Table III shows P_{esub} varies from 1/10 000 to 2/1000 of P_{erod}. On the other hand, because of the difference in the thermal expansion coefficients of Cu and glass ceramic substrates, the substrate somewhat bends in co-firing with the Cu paste on one side of the substrate. The bend of the substrate is considered to be a main cause of ΔQ_u.

TABLE III
MEASUREMENTS OF THE RELATIVE SURFACE CONDUCTIVITY σ_{sr} AND INTERFACE CONDUCTIVITY σ_{ir} FOR SINTERED COPPER FORMED ON GLASS CERAMICS BY THE CO-FIRING TECHNIQUE ($\sigma_{sr} = \sigma_s/\sigma_0$, $\sigma_{ir} = \sigma_i/\sigma_0$, $\sigma_0 = 5.8 \times 10^7$ S/m). PARAMETER $S = D/d$ IS A DIAMETER RATIO OF SUBSTRATE TO ROD AND t/H IS A THICKNESS RATIO OF SUBSTRATE TO ROD. ELECTRIC ENERGY FILLING FACTORS OF SAPPHIRE ROD AND SUBSTRATE, P_{erod} AND P_{esub}, AND GEOMETRIC FACTOR G ARE ALSO SHOWN

	Rod No.	S=D/d	t/H	f_0 (GHz)	Q_u	σ_{sr} or σ_{ir} (%)	R_s or R_i (mΩ)	$P_{erod,s}$ or $P_{erod,i}$	$P_{esub,i}$	$1/G_s$ or $1/G_i$ (Ω)
σ_s (R_s)	R1-1	3.8	—	11.762 ±0.003	6581 ±16	87.4 ±0.6	30.3 ±0.1	0.985		0.00464
	R2-1	5.6	—	17.618 ±0.005	5117 ±60	86.0 ±2.3	37.3 ±0.5	0.985		0.00477
	R3-1	6.9	—	21.724 ±0.005	4603 ±14	89.0 ±1.1	40.8 ±0.2	0.986		0.00479
	R4-1	8.8	—	27.301 ±0.002	4084 ±46	85.2 ±2.7	46.7 ±0.7	0.985		0.00467
	R5-1	11.2	—	33.687 ±0.007	3619 ±53	75.7 ±2.6	55.0 ±0.9	0.983		0.00444
σ_i (R_i)	R1-1	3.8	0.024	11.289 ±0.002	6650 ±14	78.6 ±0.6	31.3 ±0.1	0.983	0.000127	0.00446
	R2-1	5.6	0.037	16.534 ±0.002	5451 ±52	80.8 ±1.8	37.3 ±0.4	0.983	0.000400	0.00447
	R3-1	6.9	0.045	20.203 ±0.002	4951 ±19	81.3 ±1.1	41.1 ±0.3	0.982	0.000709	0.00440
	R4-1	8.8	0.056	25.010 ±0.005	4525 ±16	77.9 ±1.6	46.7 ±0.4	0.980	0.000976	0.00419
	R5-1	11.2	0.068	30.486 ±0.013	4273 ±115	74.7 ±4.7	52.7 ±1.6	0.976	0.00210	0.00387

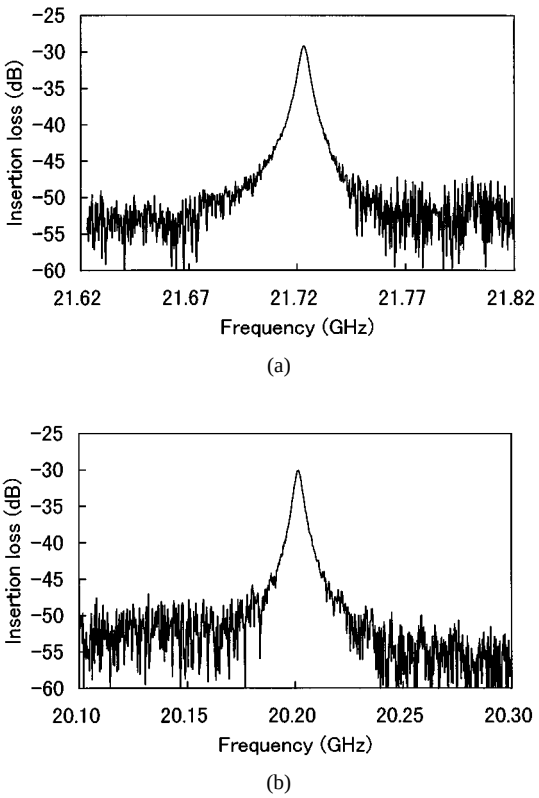

Fig. 7. Resonant peaks for: (a) surface conductivity σ_s and (b) interface conductivity σ_i measurements using sapphire rod R3-1.

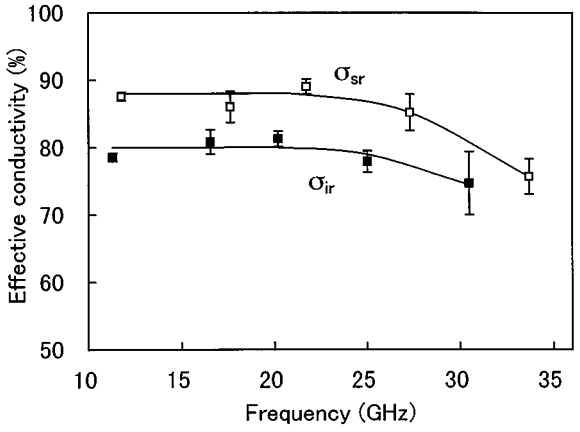

Fig. 8. Frequency dependence of relative surface conductivity σ_{sr} and relative interface conductivity σ_{ir} of sintered copper formed on the glass ceramic substrate by the co-firing technique.

E. Accuracy of FEM Calculation

The FEM analysis was used to calculate the parameters G_i, $P_{\mathrm{erod},i}$ and $P_{\mathrm{esub},i}$ in (2). We have evaluated accuracy of the FEM analysis by comparing G_s and $P_{\mathrm{erod},s}$ obtained by the FEM analysis to the values obtained from exact equations in (7)–(14) [10]. In the FEM model, the outside of the resonator for σ_s was short-circuited by a cylindrical conductive wall of diameter $d = 5D$, as shown in Fig. 9(b). Table V shows calculation results for $D = 10$ mm, $H = 5$ mm, $\varepsilon'_{\mathrm{rod}} = 9.4$, by total

TABLE IV
EVALUATION OF RANDOM ERRORS OF RELATIVE SURFACE CONDUCTIVITY AND INTERFACE CONDUCTIVITY, $\Delta\sigma_{sr}$ AND $\Delta\sigma_{ir}$, BY (27) AND (28), IN MEASUREMENTS AT 17–22 GHz. $\Delta\sigma_{Qu}$ AND $\Delta\sigma_{\tan\delta rod}$ ARE THE ERRORS OF σ_{sr} OR σ_{ir} BY STANDARD DEVIATIONS OF Q_u AND $\tan\delta_{\rm rod}$. THE $\Delta\sigma_{\tan\delta sub}$ IS CALCULATED BY $\Delta\tan\delta_{\rm sub} = 1\times10^{-4}$

	f_0 (GHz)	σ_{sr} or σ_{ir} (%)	$\Delta\sigma_{sr}$ or $\Delta\sigma_{ir}$ (%)	$\Delta\sigma_{Qu}$ (%)	$\Delta\sigma_{\tan\delta rod}$ (%)	$\Delta\sigma_{\tan\delta sub}$ (%)
σ_s	17.618	86.1	2.3	2.2	0.7	
	21.724	89.0	1.1	0.6	0.9	
σ_i	16.534	80.8	1.8	1.7	0.7	0.0
	20.203	81.2	1.1	0.7	0.9	0.0

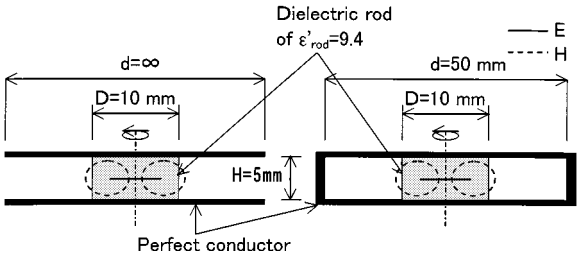

Fig. 9. Configurations of $\rm TE_{011}$ mode dielectric resonator models for comparing FEM analysis to exact analysis. (a) Exact analysis model. (b) FEM analysis model.

TABLE V
COMPARISON OF CALCULATED PARAMETERS GEOMETRIC FACTOR G_s AND ELECTRIC ENERGY FILLING FACTOR $P_{{\rm erod},s}$ OF THE DIELECTRIC ROD BY FEM WITH THOSE BY EXACT EQUATIONS (7)–(14), UNDER THE CONDITION OF $D = 10$ mm, $H = 5$ mm, $d = 50$ mm, AND $\varepsilon'_{\rm rod} = 9.4$

Parameter	FEM	Exact Eq.	Difference
f_0 (GHz)	13.5578	13.5545	0.02%
$1/G_s$ (1/Ω)	0.004433	0.004439	−0.13%
$P_{erod,s}$	0.98311	0.98321	−0.01%

mesh number of about 5000. The evaluated error is about 0.1% for $1/G_s$ and about 0.01% for $P_{{\rm erod},s}$, as shown in Table IV. These values of error are negligibly small compared with other random errors described in the previous section.

V. CONCLUSION

A microwave measurement method for the surface conductivity σ_s and interface conductivity σ_i was developed. The dielectric rod resonators were used for the measurements. Using the proposed technique, we investigated frequency dependencies of both σ_s and σ_i of a sintered copper formed on a glass ceramic substrate by the co-firing technique in the frequency range from 11 to 34 GHz. The measurement results have shown obvious difference between the values of σ_s and σ_i of the sintered copper, and their degradation with increasing frequency.

Present measurement technique will give an important information for designing and developing multi-layered substrates for high-frequency circuits, as well as a process technology to control the interface conductivity. The standard deviation $\Delta\sigma_{ir}$ of the relative interface conductivity σ_{ir} was within 5%.

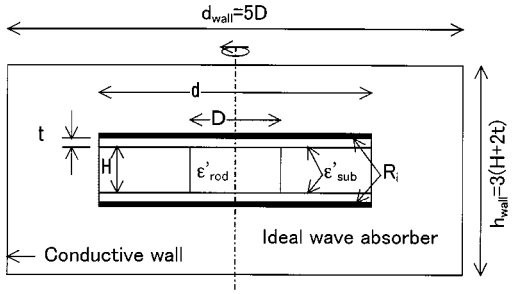

Fig. 10. Calculation model for estimation of required size ratio $S = d/D$ in the resonator for interface conductivity σ_i measurements.

APPENDIX

When $S = d/D$ is small, skin resistance R_i at interface and R_s at surface calculated by (2) and (1) have errors $\Delta R_{i,\,\rm rad}(S)$ and $\Delta R_{s,\,\rm rad}(S)$ caused by radiation loss, respectively. In the same S, the $\Delta R_{i,\,\rm rad}(S)$ is expected to be larger than $\Delta R_{s,\,\rm rad}(S)$, since the distance between two conductors for σ_i measurements is larger. We estimated the required value of S for R_i measurement, by calculating the $\Delta R_{i,\,\rm rad}(S)$ using FEM analysis. In the analysis, the resonator for R_i measurements is set in cylindrical conductive wall of no loss, as shown in Fig. 10. To estimate radiation loss, an ideal wave absorber, with relative permittivity $\varepsilon'_{\rm abs} = 1$ and loss tangent $\tan\delta_{\rm abs} = 1$, is filled in the outside d, the upper and lower side of the resonator. The diameter $d_{\rm wall}$ and height $h_{\rm wall}$ of the conductive wall is fixed to 5 times of d and 3 times of $H + 2t$, to let the field be negligibly small near the wall. The Q_u of the resonator, shown in Fig. 10, is

$$1/Q_{u,\,i}(S) = R_i/G_i(S) + P_{{\rm erod},\,i}(S)\tan\delta_{\rm rod} + P_{{\rm esub},\,i}(S)\tan\delta_{\rm sub} + P_{{\rm eabs},\,i}(S) \quad (29)$$

where $P_{\rm eabs}$ is the partial electric energy filling factor of the absorber defined as

$$P_{{\rm eabs},\,i} = \frac{W_{{\rm eabs},\,i}}{W_{et,\,i}} = \frac{\iiint_{V\rm abs}|\mathbf{E}|^2\,dv}{\iiint_{Vt}\varepsilon'(v)|\mathbf{E}|^2\,dv}. \quad (30)$$

Here, $W_{{\rm eabs},\,i}$ is the electric energy in the ideal absorber, which all dissipates as radiation loss. $W_{et,\,i}$ is defined as the total energy stored inside the conductive wall shown in Fig. 10. $P_{{\rm eabs},\,i}$ represents the reciprocal of $Q_{\rm rad}$, Q-factor by radiation loss. When S is small, (29) gives an accurate R_i from the measured value of $Q_{u,\,i}(S)$. The use of (2) in place of (29) induces an error for $\Delta R_{i,\,\rm rad}(S)$. From (2) and (29), the $\Delta R_{i,\,\rm rad}(S)$ by radiation loss is written by\rm

$$\begin{aligned}\Delta R_{i,\,\rm rad} = {} & [G_i - G_i(S)]/Q_{u,\,i}(S) \\ & + [G_i(S)P_{{\rm erod},\,i}(S) - G_iP_{{\rm erod},\,i}]\tan\delta_{\rm rod} \\ & + [G_i(S)P_{{\rm esub},\,i}(S) - G_iP_{{\rm esub},\,i}]\tan\delta_{\rm sub} \\ & + G_i(S)P_{{\rm eabs},\,i}(S). \end{aligned} \quad (31)$$

To obtain the $\Delta R_{i,\,\rm rad}(S)$, $G_i(S)$, $P_{{\rm erod},\,i}(S)$, $P_{{\rm esub},\,i}(S)$ and $P_{{\rm eabs},\,i}(S)$ are firstly calculated by FEM. Secondly, $G_i = G_i(S)$, $P_{{\rm erod},\,i} = P_{{\rm erod},\,i}(S)$ and $P_{{\rm esub},\,i} = P_{{\rm esub},\,i}(S)$ are assumed for sufficiently large S. We chose 5 as the sufficiently

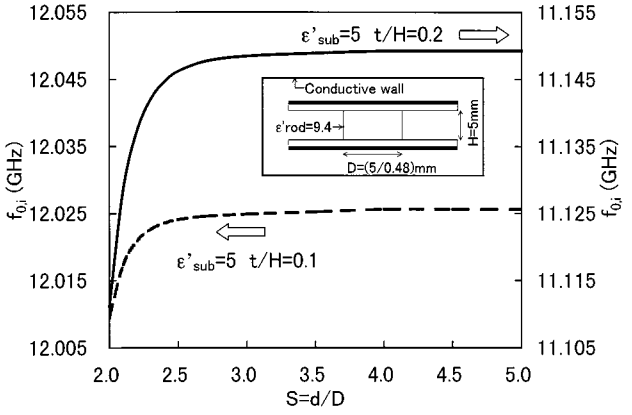

Fig. 11. Calculation of resonant frequency $f_{0,i}$ as a function of size ratio $S = d/D$, in the case of $\varepsilon'_{\rm sub} = 5$, $t/H = 0.1$ and 0.2. The calculation model is illustrated in the figure.

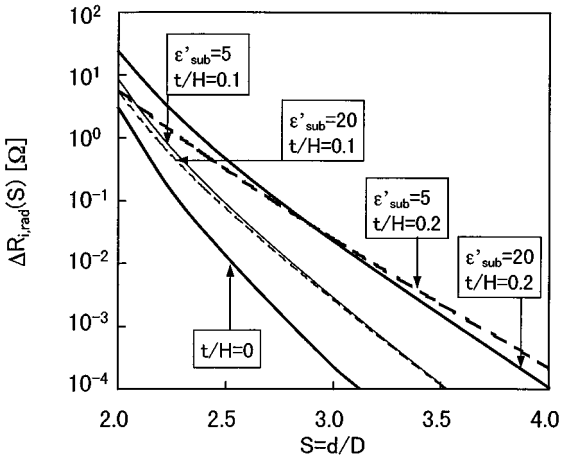

Fig. 12. Calculation of error of skin resistance at interface $\Delta R_{i,\,\rm rad}(S)$ by radiation loss as a function of size ratio $S = d/D$, for $\varepsilon'_{\rm rod} = 9.4$ and $H/D = 0.48$ in the model shown in Fig. 10.

large S, since calculation of the resonant frequency $f_{0,i}(S)$ was fully saturated at $S = 5$, as shown in Fig. 11. The calculation of $f_{0,i}(S)$ was performed for $\varepsilon'_{\rm rod} = 9.4$ $\varepsilon'_{\rm sub} = 5.0$, $H = 5$ mm and $H/D = 0.48$, corresponding to the experimental conditions of present study. Then, $Q_{u,i}(S)$ is calculated by (29), using typical values of R_i, $\tan\delta_{\rm rod}$, and $\tan\delta_{\rm sub}$. Finally, $\Delta R_{i,\,\rm rad}(S)$ is obtained by (31), using $Q_{u,i}(S)$.

Fig. 12 shows the calculated results of $\Delta R_{i,\,\rm rad}(S)$ for R_i corresponding to $\sigma_i = \sigma_0 = 5.8 \times 10^7/\Omega$m, with the conditions: $\varepsilon'_{\rm rod} = 9.4$, $\varepsilon'_{\rm sub} = 5$, 20, $t/H = 0$, 0.1, 0.2, $H = 5$ mm and $H/D = 0.48$, $\tan\delta_{\rm rod} = 1 \times 10^{-5}$ and $\tan\delta_{\rm sub} = 1 \times 10^{-3}$. The results of $\Delta R_{i,\,\rm rad}(S)$ for $t/H = 0$ in Fig. 12 correspond to $\Delta R_{s,\,\rm rad}(S)$, which is an error of skin resistance of surface side by radiation. Obtained values of $\Delta R_{i,\,\rm rad}(S)$ shown in Fig. 12 do not depend on R_i, $\tan\delta_{\rm rod}$ and $\tan\delta_{\rm sub}$, since the first three terms in (31) are negligibly small and the last term in (31) mainly determines the values of $\Delta R_{i,\,\rm rad}(S)$ under the actual condition of $\sigma_i > 0.58 \times 10^7/\Omega$m, $\tan\delta_{\rm rod} < 1 \times 10^{-3}$ and $\tan\delta_{\rm sub} < 1 \times 10^{-2}$. Furthermore, the values of $\Delta R_{i,\,\rm rad}(S)$ in Fig. 12 do not depend on the size of the resonator when the resonator keeps ratios of D/H, $S = d/D$, and t/H, since the last term of (31) is determined not by the size itself, but the size ratio of the resonator. This is attributable to the fact that the partial electric energy factor P_e and the geometric factor G depend not on the size, but the size ratio of the resonator. $S = d/D$ must be set to satisfy $\Delta R_{i,\,\rm rad}(S) < 0.1$ mΩ, since the measuring error of R_i is less than about 1 mΩ in the present method. From Fig. 12, we conclude that $S > 3.5$ and $S > 4.0$ are required for $t/H = 0.1$ and $t/H = 0.2$, respectively, in the case of $\varepsilon'_{\rm sub} = 5$.

REFERENCES

[1] Y. Kobayashi and J. Sato, "Complex permittivity measurement of dielectric plates by a cavity resonance method," IEICE, Tokyo, Japan, IEICE Tech. Rep. MW88-40, pp. 43–50, Nov. 1988.

[2] ——, "Improved cavity resonance method for nondestructive measurement of complex permittivity of dielectric plate," in *CPEM Dig.*, 1988, pp. 147–148.

[3] G. Kent, "Nondestructive permittivity measurement of substrates," *IEEE Trans. Instrum. Meas.*, vol. 45, pp. 102–106, Feb. 1996.

[4] G. Kent and S. Bell, "The gap correction for the resonant-mode dielectrometer," *IEEE Trans. Instrum. Meas.*, vol. 45, pp. 98–101, Feb. 1996.

[5] A. Nakayama, "A measurement method of complex permittivity at pseudo micro wave frequency using a cavity resonator filled with dielectric material," *IEICE Trans. Electron.*, vol. E77-C, no. 6, pp. 894–899, June 1994.

[6] A. Nakayama, A. Fukuura, and M. Nishimura, "Complex permittivity measurement at pseudo microwave frequency using a dielectric-plate-loaded cavity resonator," *IEICE Trans. Electron.*, vol. E80-C, no. 8, pp. 1117–1125, Aug. 1997.

[7] J. Baker-Jarvis, R. G. Geyer, J. H. Grosvenor, M. D. Janezic, C. A. Jones, B. Riddle, C. M. Weil, and J. Krupka, "Dielectric characterization of low-loss materials, a comparison of techniques," *IEEE Trans. Dielect. Elect. Insulation*, vol. 5, pp. 571–577, Aug. 1998.

[8] H. Tanaka and F. Okada, "Precise measurements of dissipation factor in microwave printed circuit boards," *IEEE Trans. Instrum. Meas.*, vol. 38, pp. 509–514, Apr. 1989.

[9] J. Krupka and J. Mazierska, "Single-crystal dielectric resonators for low-temperature electronics applications," *IEEE Trans. Microwave Theory Tech.*, vol. 48, pp. 1270–1274, July 2000.

[10] B. W. Hakki and P. D. Coleman, "A dielectric resonator method of measuring inductive capacities in the millimeter range," *IRE Trans. Microwave Theory Tech.*, vol. MTT-8, pp. 402–410, July 1960.

[11] Y. Kobayashi and M. Katoh, "Microwave measurement of dielectric properties of low-loss materials by the dielectric rod resonator method," *IEEE Trans. Microwave Theory Tech.*, vol. MTT-33, pp. 586–592, July 1985.

[12] Y. Kobayashi and H. Tamura, "Round robin test on a dielectric resonator method for measuring complex permittivity at microwave frequency," *IEICE Trans. Electron.*, vol. E77-C, no. 6, pp. 882–887, June 1994.

[13] Y. Terashi, "Development of material for multilayer ceramic substrate with copper wiring in millimeter wave applications," in *IEMT/IMC Symp.*, Apr. 2000, pp. 382–385.

Akira Nakayama was born in Kyoto, Japan, on March 14, 1957. He received the B.S. degree from Osaka City University, Osaka, Japan, in 1981 and the M.S. degree from Kobe University, Kobe, Japan, in 1983, both in earth science.

In 1983, he joined Kyocera Corporation, Kagoshima, Japan. He has been engaged in the development of microwave and millimeter-wave measurement techniques for physical properties of materials.

Mr. Nakayama is a member of the Institute of Electronics, Information and Communication Engineers (IEICE), Japan, and the Ceramic Society of Japan (CSJ).

Yoshitake Terashi was born in Kumamoto, Japan, on November 14, 1965. He received the B.S. degree in applied chemistry from the Nagoya Institute of Technology, Nagoya, Japan, in 1990.

In 1990, he joined Kyocera Corporation, Kagoshima, Japan. He has been engaged in the development of material for multilayer ceramic substrates in microwave and millimeter-wave applications.

Hiroshi Uchimura was born in Shizuoka, Japan, in 1959. He received the B.S. and M.S. degrees in physics from Kagoshima University, Kagoshima, Japan, in 1983 and 1985, respectively.

From 1985 to 1989, he was with the Hitachi Engineering Corporation, where he worked on the compression of pictures for facsimile. In 1989, he joined the Kyocera Corporation, Kagoshima, Japan. From 1989 to 1995, he worked on fracture mechanics of ceramics. Since 1995, he has been engaged in the research and development on package and antenna for millimeter-wave modules.

Atsuomi Fukuura (M'97) was born in Hokkaido, Japan, on January 30, 1966. He received the M.S. degree in physics from Kwansei Gakuin University, Nishinomiya, Japan, in 1990, and the M.Eng. degree in electrical engineering from McMaster University, Hamilton, ON, Canada, in 1999.

Since he joined Kyocera Corporation, Kagoshima, Japan, in 1990, he has been engaged in numerical techniques for the analysis and design of microwave components. His current interest includes components for wireless and optical communications.